Asian Journal of Chemistry; Vol. 34, No. 5 (2022), 1291-1296

ASIAN JOURNAL OF CHEMISTRY

https://doi.org/10.14233/ajchem.2022.23670

Design and Study of Silk Cocoon-ZnO Micro-Nanocomposite based Gas Sensor for Detection of Flammable Gas at Room Temperature

SINDHU SREE MURALIDHAR[1], MURTHY MUNIYAPPA[2], MAHESH SHASTRI[2], VINAY GANGARAJU[1], NAVYARANI MARLINGAIAH[3], C.S. ANANDA KUMAR[1], PRASANNA D. SHIVARAMU[1] and DINESH RANGAPPA[1,*]

[1]Department of Applied Sciences (Nanotechnology), Visvesvaraya Technological University, Center for Post Graduate Studies, Muddenahalli, Chikkaballapur-562101, India
[2]Department of Electronics and Communications, Nagarjuna College of Engineering and Technology, Devanahalli, Bangalore-562164, India
[3]Department of Applied Sciences, Dayanand Sagar University, Kumar Swamy Layout, Bengaluru-560111, India

*Corresponding author: E-mail: dineshrangappa@gmail.com, dinesh.rangappa@vtu.ac.in

Received: 12 December 2021; *Accepted*: 10 March 2022; *Published online*: 20 April 2022; AJC-20785

In present work, a simple hydrothermal method is employed for the synthesis of silk cocoon-ZnO micro-nanocomposite and investigation of their gas sensing is reported. The ZnO nanoparticles were synthesized using hydrothermal methods and coated on the surface of silk cocoon layers using a simple doctor-blade method. The as-prepared silk cocoon-ZnO micro-nanocomposite materials were analyzed using X-ray diffractometer (XRD), scanning electron microscopy (SEM) and Fourier transform infrared spectroscopy (FTIR) and IV characteristics. The results confirm the formation of pure ZnO and silk cocoon-ZnO micro-nanocomposite with rod-like morphology. The surface of silk cocoon fibers was uniformly coated with ZnO nanorods. The gas sensing property of the as-prepared silk cocoon-ZnO micro-nanocomposite was evaluated against the leakage of LPG gas at room temperature. Voltage-Time curve analysis was performed and found that with the detection of LPG gas there is an increase in the voltage. Based on the present findings, it is proposed that silk cocoon-ZnO micro-nanocomposite based devices will be suitable for light weight, biocompatible and low-cost gas sensors.

Keywords: Silk cocoon fibers, ZnO nanorods, Hydrothermal method, Micro-nanocomposite, Gas sensor.

INTRODUCTION

The rapid expansion of industrialization and the increased urban population have led to a rise in air pollution. The air pollution due to industrial and automobile exhausts gases that have caused this pollution. This process has created major health challenges for living organisms [1]. Therefore, to maintain sustainable development and balance the ecosystem, there is a necessity for a clean air supply. On the other hand, with the continued industrialization, many industries have a drawback of leakage inflammable and explosive gases into the environment [2]. Hence, there is an urge to develop accurate real time gas monitoring sensors to clean and detect pollutants. In recent times, gas sensors have been used in various fields like mining industries (for methane detection) [3], fuel cells (for hydrogen gas detection) [4], fertilizer industries (for NH_3 detection) [5] and oil refineries (for hydrocarbon detection) [6].

Therefore, a highly sensitive, small size, low cost and reliable gas sensor development to detect the toxic and explosive gasses at room temperature with continuous monitoring is the need of the time [7,8]. For last few decades, researchers have developed metal oxide semiconductor-based gas sensors to meet the above requirements [9-14]. Recently, nanomaterial based gas sensors have shown a higher sensitivity than bulk material. This is due to their high surface area and small size [15]. Hence many types of metal oxide based nanomaterial gas sensors have been developed that include SnO_2, TiO_2, CuO, Fe_2O_3, ZnO and WO_3 [15-22]. Among them, the ZnO nanomaterial has been emerging as one of the promising materials for gas sensing applications [16,17].

The ZnO nanomaterial is an intrinsic n-type semiconductor having a bandgap of 3.37 eV [14,23]. These ZnO nanostructure has been synthesized by various methods like chemical vapour deposition, sol-gel method, RF sputtering, hydrothermal

and molecular beam deposition [24-31]. It possesses different morphologies like 1-D, 2-D, and 3-D nanostructures [32-34]. Among them, urchins are 3D nanostructures. The 2D nanostructures are nanosheets, nanoplates, whereas the nanowire and nanorods are 1D nanostructures.

Recently, the ZnO composite with polymer materials has opened up an opportunity for the development of biomaterial-based gas sensors. A polymer/ZnO composite based hybrid solar cell was reported by Venkatesan *et al*. [35]. They synthesized bilayer interfaces of ZnO films with cationic polymer modification (PEIE) and found that the enhanced device lifetime for PEIE modified ZnO as compared to pristine ZnO. However, the drawback of ZnO-based gas sensors is that they have to be operated in high temperatures of 200 and 500 ºC for activation. So far, less research work was carried out related to the development of biomaterial based gas sensors operated at room temperature.

Our interest has deployed silk cocoons as a biomaterial for gas sensing applications. Silk cocoon is two protein-polymer materials, a highly porous network. Many studies have been reported on silk cocoons as a suitable material for gas sensing because of their porosity and crystal structure. Naturally, this silk cocoon possesses a controlled gas permeability property for the protection of worms inside it. This allows only oxygen and filters the carbon dioxide inside the matrix [36-38]. In this work, a simple silk cocoon fiber-ZnO based gas sensor operated at room temperature is developed. The gas sensing property was analyzed using LPG gas.

EXPERIMENTAL

Silk cocoons were procured from a central silk board, Bengaluru, India. Sodium hydroxide and zinc nitrate ($Zn(NO_3)_2 \cdot 6H_2O$) were purchased from Sigma-Aldrich. All chemicals were of analytical grade and used without any further modification.

Preparation of ZnO and silk cocoon-ZnO composite: The hydrothermal method was used for the synthesis of ZnO nanoparticles. A 30 mL 0.5 M $Zn(NO_3)_2 \cdot 6H_2O$ was added to 30 mL of 5 M NaOH and stirred for 1h. The solution is now transferred to a Teflon and kept in hydrothermal at temperature 100 ºC for 2 h. The obtained powder was cooled and grinded for 30 min. A 2 mg of as-synthesized ZnO nanoparticles were gently grinded for 5 min by adding distilled water to maintain a slurry formation. To this slurry, a layer of silk cocoon (a small piece of 1 cm × 1cm size) was added and grinded for the next 10 min. Thus, the ZnO nanoparticles were deposited on the surface of the silk cocoon layer and formed silk cocoon-ZnO micro-nanocomposite. Further, it was dried at room temperature and used for the characterization.

Characterization: The surface morphology and elemental analysis of ZnO and silk cocoon-ZnO micro-nanocomposite were observed by scanning electron microscopy (SEM, Hitachi SU1510). X-ray diffraction (XRD Rigaku IV), analysis of as-prepared samples were performed using Cu$K\alpha$1 radiation operated with 2θ diffraction angle at 35 kV and 25 mA from 10 to 80º with a step width of 0.02º. The surface functional group analysis was performed using Fourier transform infrared spectroscopy (Perkin-Elmer STA8000). An electrochemical workstation (Keithley 2400 SMU model) was employed to analyze the electrical characteristic curves.

RESULTS AND DISCUSSION

Structural analysis: The structural analysis of ZnO and silk cocoon-ZnO micro-nanocomposite has been analyzed using the XRD pattern as shown in Fig. 1. It is observed that ZnO nanoparticle has a *hkl* plane of (100), (002), (101), (102), (110), (103), (200), (112) and (201) represents the wurtzite crystal structure. These XRD patterns peaks were matched to the JCPDS card number 36-1451. The as-synthesized ZnO nanoparticles were deposited on the silk cocoon layer using the doctor-blade technique. It is noticed in the XRD pattern of silk cocoon--ZnO micro-nanocomposite that along with the ZnO characteristic peaks, a diffraction peak at 20.6º is also found, which has an *hkl* plane of (020) and represents the β-sheet crystalline structure of the silk cocoon. Thus, it is concluded the formation of silk cocoon-ZnO micro-nanocomposite.

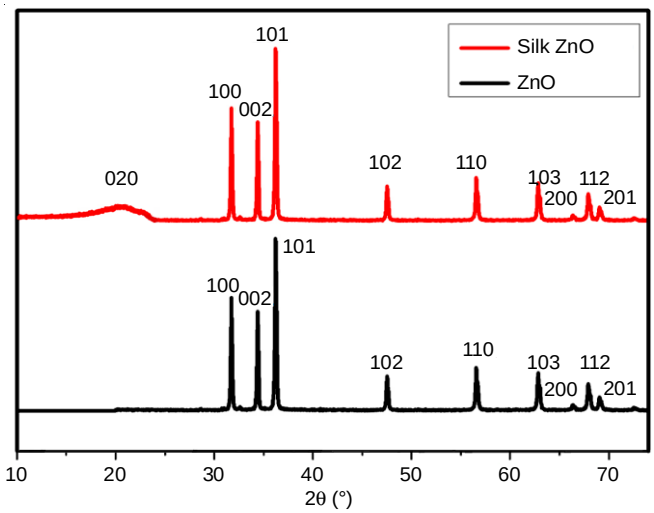

Fig. 1. XRD patterns of ZnO (black) and Silk-ZnO micro-nanocomposite (red) representing the crystal structure

The morphology of ZnO and silk cocoon-ZnO micro-nanocomposite was analyzed using SEM technique. The as-synthesized ZnO nanoparticles showed a rod-like shape morphology (Fig. 2a). The uniformed shape of ZnO nanoparticles can be noticed, whereas,Fig. 2b shows the bare silk cocoon fiber matrix and can observe the fibers with irregular porosity formation. Using the doctor-blade method the ZnO nanoparticles were deposited on the silk cocoon fiber matrix. Fig. 2c shows the ZnO nanoparticles are uniformly deposited on the surface of fiber-matrix and thus forming a closed network. After the deposition process, a change in the fiber surface can be noticed in Fig. 2d. Thus with the proposed method, there is a possibility of uniform deposition on the surface of the silk cocoon fiber matrix.

Electrical measurement for gas sensing analysis: The electrical measurements were performed on ZnO nanoparticles and silk cocoon-ZnO micro-nanocomposite. Here, LPG gas was used in this analysis, which was carried out at room temperature. Fig. 3a shows the change of resistance with respect to

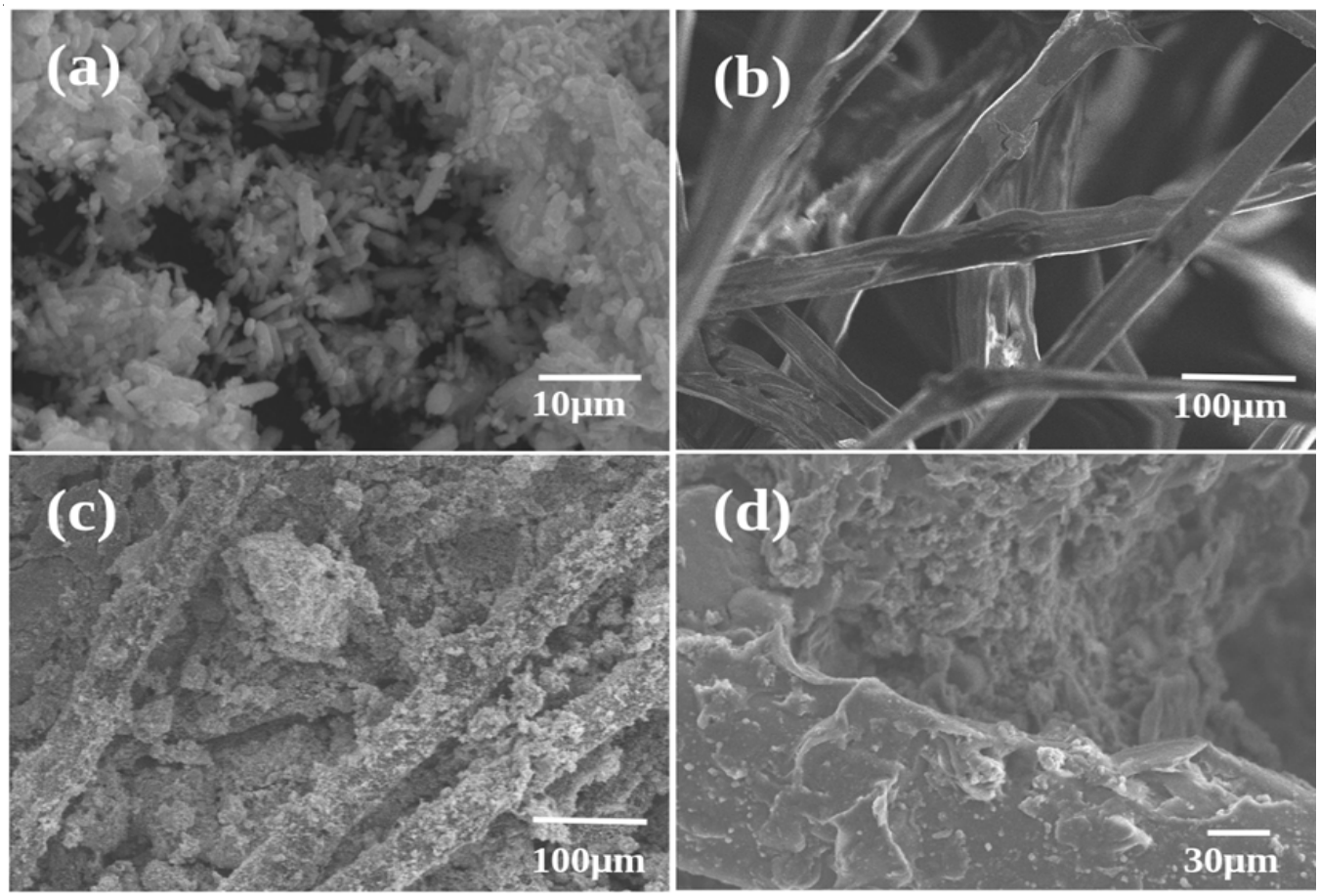

Fig. 2. SEM image of (a) ZnO nanorods, (b) bare silk cocoon fiber matrix, (c) ZnO nanorods deposited on the silk cocoon fiber matrix, and (d) silk-ZnO micro-nanocomposite and shows the uniform deposition of ZnO nanoparticles on the surface of the silk cocoon fiber matrix

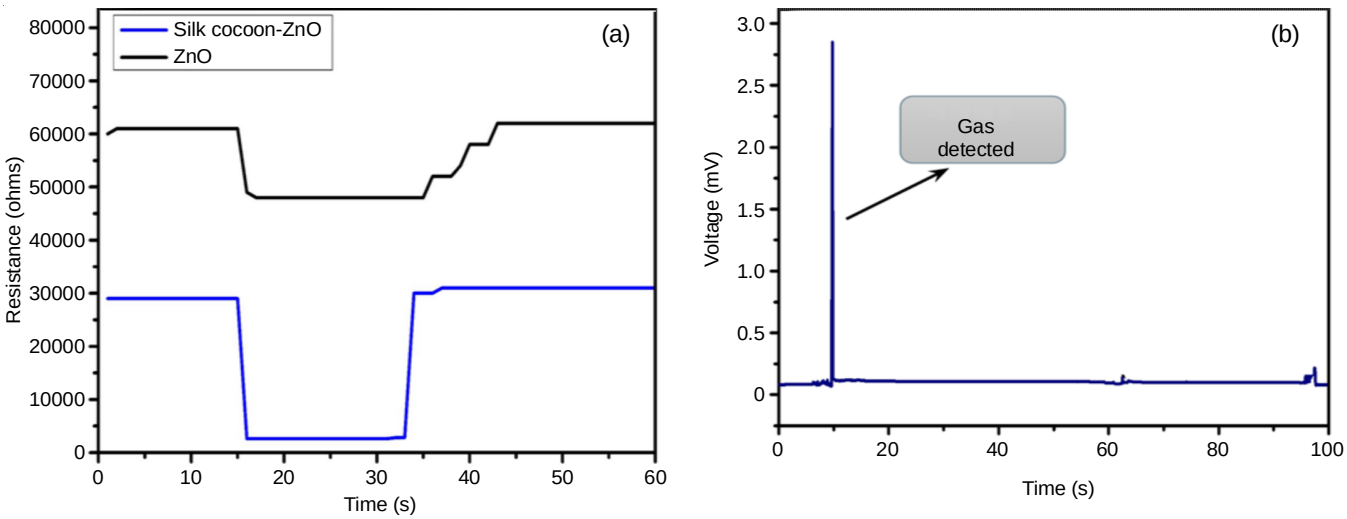

Fig. 3. Electrical measurements of ZnO and silk cocoon-ZnO micro-nano composite: (a) resistance - time curve of ZnO and silk cocoon-ZnO micro nanocomposite and (b) voltage-time curve of silk cocoon-ZnO micro nanocomposite detection agonist the LPG gas

the time when the sample was exposed to LPG gas. It is noticed that with exposure to gas there is a decrease in resistance in both ZnO and silk cocoon-ZnO micro nanocomposite. This indicates the detection of LPG gas. However, it is clearly observed that the silk cocoon-ZnO micro nanocomposite has shown a better response than the ZnO nanoparticle. This is due to that the gas molecules have interacted with the oxygen cites of silk cocoon-ZnO micro-nanocomposite and thereby change in the resistance is observed. It is obvious that with the decrease in resistance, there is an increase in the voltage as shown in

Fig. 3b. The sharp peak indicates the detection of LPG gas, where the voltage has been increased from 0.3 mV to 2.8 mV. Based on the findings, it is notified that the gas molecules are trapped on the surface of the composite and form a closed network, which facilitates the transformation of ions or electrons in the composite matrix.

FTIR studies: Functional group analysis was performed for silk cocoon-ZnO micro-nanocomposite before and after exposure to LPG gas. The analyses were performed for the spectral range from 4000 cm^{-1} to 400 cm^{-1}. The regions from 2000-400 cm^{-1} show the fingerprint region of silk-cocoon-ZnO micro-nanocomposite. Specifically, the absorption peak at 575.9 cm^{-1} shows the stretching vibration of ZnO in vibration mode (Fig. 4). The peaks at 1005.3, 1118.1, 1355.5 and 1383.7 cm^{-1} belong to the stretching vibration of C-N bonds of the primary amine group of silk fiber and also the secondary alcohol-plane vibration [39]. It is clearly observed from the spectra that there is no change in the fingerprint region before and after LPG gas exposure. This shows that no structural deformation occurs even after the detection of gas. However, a change in C-C bond has been noticed in the 2345.2 cm^{-1}, which may be due to the interaction of gas molecules to the polymer hydrogen chain of the composite.

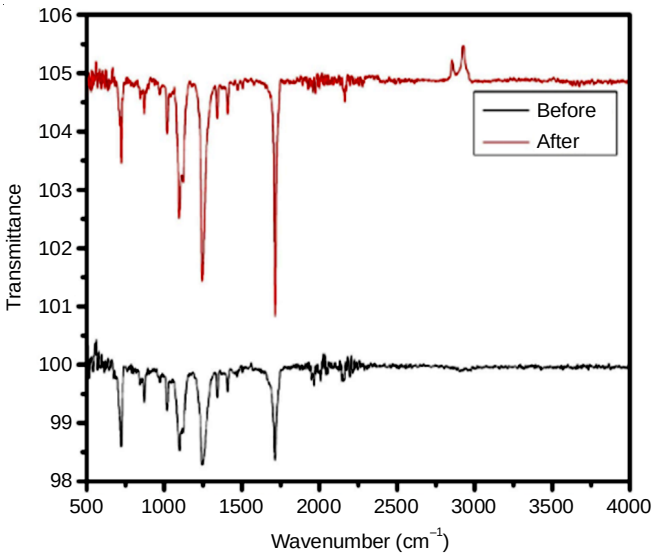

Fig. 4. Functional group (FTIR) spectral analysis of Silk-ZnO composite before and after gas exposure

Gas response and sensing mechanism: Additionally, the performance of ZnO nanoparticles and silk cocoon-ZnO micro nanocomposite against the exposure of LPG gas were also analyzed. Fig. 5 shows the response (ΔR) - time curve of both ZnO and Silk cocoon-ZnO. It is clearly noticed that an increase in the response indicates the LPG gas detected and in contract decrease in response shows no detection of LPG gas. The response of ZnO is very low with respect to the silk cocoon-ZnO micro- nanocomposite (same has been highlighted in the figure). Though ZnO has the tendency to detect toxic gas, its performance has been further increased with silk cocoon composite.

The response (ΔR) was calculated using the following equation:

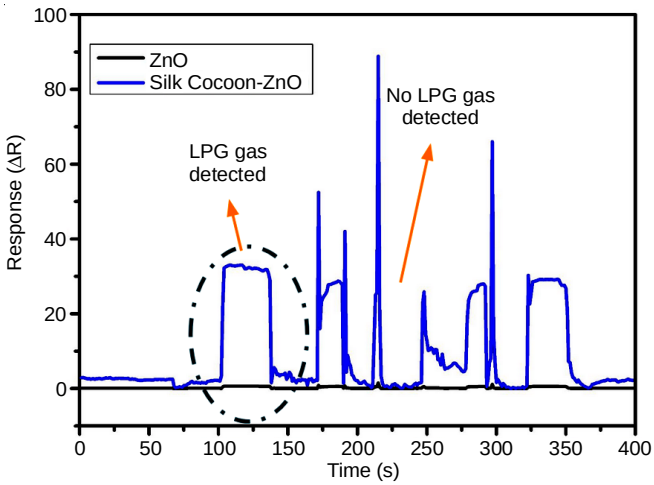

Fig. 5. Response (ΔR) - time curve analysis of ZnO nanoparticle (black) and silk cocoon-ZnO micro nanocomposite (blue) against the detection of LPG gas

$$\Delta R = \frac{R_a - R_g}{R_a}$$

where R_a and R_g represent the atmospheric gas and LPG gas detected resistance, respectively.

Fig. 6 shows the possible gas sensing mechanism of silk cocoon-ZnO micro-nanocomposite. Generally, the gas sensing sensitivity relies on the depletion layer of the sample. Here, when LPG gas is exposed to the surface of silk cocoon-ZnO micro-nanocomposite, the oxygen molecules is adsorbed on the surface of the composite in the presence of atmospheric gas. The oxygen molecules binding to the surface of silk cocoon-ZnO micro-nanocomposite will extract the electrons from the valence band to the conduction band [40]. This leads to the formation of a conduction medium and thereby an increase in voltage is observed. Further, based on the band bending theory, the bandgap of silk cocoon-ZnO micro-nanocomposite moves upwards due to the high electronegativity of oxygen molecules under atmospheric air [8]. Thus results in the bandgap of 4.18 eV as shown in Fig. 6.

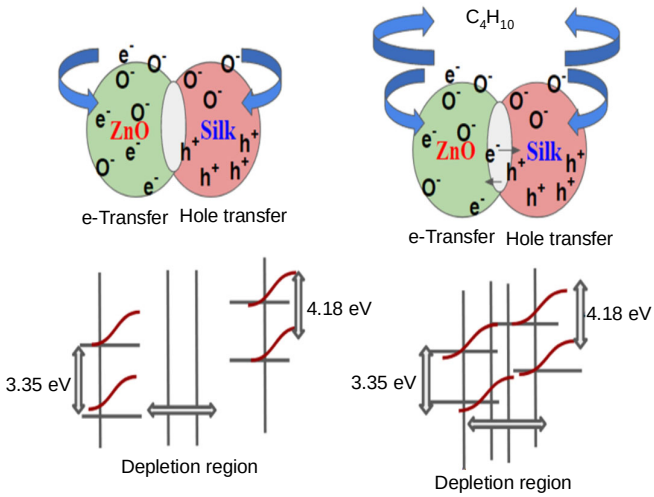

Fig. 6. Graphical representation of gas sensing mechanism of silk-ZnO composite before and after LPG gas exposure

Hence LPG gas is a mixture of more than 20 hydrocarbon groups. Generally, when the reductive gasses like NH_3, HCHO, and CH_4 have interacted with the ZnO surface, there will be a decrease in the resistance. This is due to the oxygen ions donating free electrons to the conduction band of ZnO and thereby decreasing the barrier height. However a contrasting behaviour can also be noticed that with the interaction with gasses like NO_2 and CO_2, there will be an increase in the resistance [8,33]. Based on the results, it is concluded that the NO_2 and CO_2 molecules of LPG gas have interacted with the surface of the nanocomposite, and hence thereby a formation of conducting medium was observed.

In addition, the sensitivity and sensor time response of the silk cocoon-ZnO micro-nanocomposite was calculated using the following formula and found to be 0.05 kΩ s^{-1}.

Here, the sensitivity (S) is defined as the ratio change in the resistance in air and in the gas normalizes to the exposure time:

$$S = \frac{R}{T} M\Omega/s$$

where R is the change of resistance in atmospheric air and T is the change with respect to time.

Comparative studies: Table-1 shows the comparison of the ZnO nanocomposite as gas sensing material for gas sensor. No much literature report has been found for polymer based ZnO composite for LPG gas detection at room temperature. It is clearly observed that the ZnO operated temperature between 200 to 500 ºC has shown a good response. However, silk cocoon-ZnO micro-nanocomposite based gas sensor has shown high response than other materials. Thus, present findings concludes that the proposed method can be used as a gas sensor at room temperature.

TABLE-1
COMPARISON TABLE OF VARIOUS ZnO COMPOSITE AS GAS SENSING MATERIAL, AGAINST THE LPG GAS

Sensor	Temp. (°C)	Response	Ref.
ZnO-CuO (80)	300	87.3	[41]
ZnO-Al (94)	325	89.0	[42]
ZnO-Cu (106)	500	0.9	[43]
ZnO nanorods (46)	340	5.0	[44]
Porous ZnO nanotubes	200	8.0	[45]
Silk cocoon-ZnO	RT	92.6	This work
ZnO nanorods	RT	61.1	This work

Conclusion

In this work, a gas sensing property of silk cocoon-ZnO composite at room temperature has been studied. The novel nanocomposite has been prepared using a simple doctor blade method. The ZnO nanoparticles were synthesized using hydrothermal methods and obtained rod-like morphology. Using band bending theory, we have analyzed the barrier height of silk cocoon-ZnO micro-nanocomposite after sensing the gas. These results indicated that with the detection of LPG gas there is an increase in the voltage. Thus, based on the present findings this approach is suitable for industries like mining, fuel cells, oil refiners and fertilization industries.

CONFLICT OF INTEREST

The authors declare that there is no conflict of interests regarding the publication of this article.

REFERENCES

1. V.S. Bhati, M. Hojamberdiev and M. Kumar, *Energy Rep.*, **6(Suppl. 4)**, 46 (2020); https://doi.org/10.1016/j.egyr.2019.08.070
2. T. Hübert, L. Boon-Brett, G. Black and U. Banach, *Sens. Actuators B Chem.*, **157**, 329 (2011); https://doi.org/10.1016/j.snb.2011.04.070
3. P. Bhattacharyya, P.K. Basu, H. Saha and S. Basu, *Sens. Actuators B Chem.*, **124**, 62 (2007); https://doi.org/10.1016/j.snb.2006.11.046
4. F.J. Sansone, *Marine Chem.*, **37**, 3 (1992); https://doi.org/10.1016/0304-4203(92)90053-D
5. R. Ghosh, A. Midya, S. Santra, S.K. Ray and P.K. Guha, *ACS Appl. Mater. Interfaces*, **5**, 7599 (2013); https://doi.org/10.1021/am4019109
6. D.J. Wales, J. Grand, V.P. Ting, R.D. Burke, K.J. Edler, C.R. Bowen, S. Mintova and A.D. Burrows, *Chem. Soc. Rev.*, **44**, 4290 (2015); https://doi.org/10.1039/C5CS00040H
7. Ü. Özgür, Y.I. Alivov, C. Liu, A. Teke, M.A. Reshchikov, S. Dogan, V. Avrutin, S.J. Cho and H.A. Morkoç, *J. Appl. Phys.*, **98**, 041301 (2005); https://doi.org/10.1063/1.1992666
8. A. Dey, *Mater. Sci. Eng. B*, **229**, 206 (2018); https://doi.org/10.1016/j.mseb.2017.12.036
9. S.H. Hahn, N. Barsan, U. Weimar, S.G. Ejakov, J.H. Visser and R.E. Soltis, *Thin Solid Films*, **436**, 17 (2003); https://doi.org/10.1016/S0040-6090(03)00520-0
10. X. He, J. Li, X. Gao and L. Wang, *Sens. Actuators B Chem.*, **93**, 463 (2003); https://doi.org/10.1016/S0925-4005(03)00205-3
11. B. Shouli, D. Li, D. Han, R. Luo, A. Chen and C.L. Chung, *Sens. Actuators B Chem.*, **150**, 749 (2010); https://doi.org/10.1016/j.snb.2010.08.007
12. G. Korotcenkov, V. Brinzari, V. Golovanov and Y. Blinov, *Sens. Actuators B Chem.*, **98**, 41 (2004); https://doi.org/10.1016/j.snb.2003.08.022
13. J. Zhang, Z. Qin, D. Zeng and C. Xie, *Phys. Chem. Chem. Phys.*, **19**, 6313 (2017); https://doi.org/10.1039/C6CP07799D
14. Z.L. Wang, *ACS Nano*, **2**, 1987 (2008); https://doi.org/10.1021/nn800631r
15. Y. Zhang, D. Li, L. Qin, P. Zhao, F. Liu, X. Chuai, P. Sun, X. Liang, Y. Gao, Y. Sun and G. Lu, *Sens. Actuators B Chem.*, **255**, 2944 (2018); https://doi.org/10.1016/j.snb.2017.09.115
16. J. Zhang, Z. Zhu, C. Chen, Z. Chen, M. Cai, B. Qu, T. Wang and M. Zhang, *Nanotechnology*, **29**, 275501 (2018); https://doi.org/10.1088/1361-6528/aabd72
17. P. Dwivedi, N. Chauhan, P. Vivekanandan, S. Das, D.S. Kumar and S. Dhanekar, *Sens. Actuators B Chem.*, **249**, 602 (2017); https://doi.org/10.1016/j.snb.2017.03.154
18. B. Urasinska-Wojcik, T.A. Vincent, M.F. Chowdhury and J.W. Gardner, *Sens. Actuators B Chem.*, **239**, 1051 (2017); https://doi.org/10.1016/j.snb.2016.08.080
19. A. Umar, A.A. Alshahrani, H. Algarni and R. Kumar, *Sens. Actuators B Chem.*, **250**, 24 (2017); https://doi.org/10.1016/j.snb.2017.04.062
20. P. Rai, Y.-S. Kim, H.-M. Song, M.-K. Song and Y.-Y. Yu, *Sens. Actuators B Chem.*, **165**, 133 (2012); https://doi.org/10.1016/j.snb.2012.02.030
21. J. Zheng, Z.-Y. Jiang, Q. Kuang, Z.-X. Xie, R.-B. Huang and L.-S. Zheng, *J. Solid State Chem.*, **182**, 115 (2009); https://doi.org/10.1016/j.jssc.2008.10.009
22. S. Ameen, M.S. Akhtar, M. Song and H.S. Shin, *ACS Appl. Mater. Interfaces*, **4**, 4405 (2012); https://doi.org/10.1021/am301064j

23. C. Baratto, *RSC Adv.*, **8**, 32038 (2018); https://doi.org/10.1039/C8RA05357J
24. Q. Yang, Z. Lu, J. Liu, X. Lei, Z. Chang, L. Luo and X. Sun, *Prog. Nat. Sci.*, **23**, 351 (2013); https://doi.org/10.1016/j.pnsc.2013.06.015
25. K. Mondal and A. Sharma, *RSC Adv.*, **6**, 94595 (2016); https://doi.org/10.1039/C6RA21477K
26. R. Sui and P. Charpentier, *Chem. Rev.*, **112**, 3057 (2012); https://doi.org/10.1021/cr2000465
27. Y. Boyjoo, M. Wang, V.K. Pareek, J. Liu and M. Jaroniec, *Chem. Soc. Rev.*, **45**, 6013 (2016); https://doi.org/10.1039/C6CS00060F
28. G. Niu, G. Saint-Girons and B. Vilquin, Eds.: M. Henini, Epitaxial Systems Combining Oxides and Semiconductors, In: Molecular Beam Epitaxy, Elsevier, Ed.: 2, Chap. 17, pp. 377-402 (2018).
29. D. Nunes, A. Pimentel, L. Santos, P. Barquinha, L. Pereira, E. Fortunato and R. Martins, Synthesis, Design and Morphology of Metal Oxide Nanostructures, Elsevier, pp. 21-57 (2019).
30. W. Wang, Z. Li, W. Zheng, H. Huang, C. Wang and J. Sun, *Sens. Actuators B Chem.*, **143**, 754 (2010); https://doi.org/10.1016/j.snb.2009.10.016
31. W. Wang, Z. Li, W. Zheng, H. Huang, C. Wang and J. Sun, *Sens. Actuators B Chem.*, **143**, 754 (2010); https://doi.org/10.1016/j.snb.2009.10.016
32. C. Wang, L. Yin, L. Zhang, D. Xiang and R. Gao, *Sensors*, **10**, 2088 (2010); https://doi.org/10.3390/s100302088
33. S. Venkatesan, E. Ngo, D. Khatiwada, C. Zhang and Q. Qiao, *ACS Appl. Mater. Interfaces*, **7**, 16093 (2015); https://doi.org/10.1021/acsami.5b04687
34. P.K. Ghosh and A. Sarkar, Silk Cocoon and Rubber based Gas Sensors, Proceedings of the International Conference on Sensing Technology, ICST, pp. 121-125 (2012); https://doi.org/10.1109/ICSensT.2012.6461653
35. Y. Qi, H. Wang, K. Wei, Y. Yang, R.-Y. Zheng, I.S. Kim and K.-Q. Zhang, *Int. J. Mol. Sci.*, **18**, 237 (2017); https://doi.org/10.3390/ijms18030237
36. X. Liu and K. Zhang, Silk Fiber-Molecular Formation Mechanism, Structure-Property Relationship and Advanced Applications, In: Oligomerization of Chemical and Biological Compounds, IntechOpen (2014); https://doi.org/10.5772/57611
37. N.B. Thakare, F.C. Raghuwanshi, V.S. Kalyamwar and Y.S. Tamgadge, *AIP Conf. Proc.*, **1953**, 030057 (2018); http://doi.org/10.1063/1.5032392
38. N Jayarambabu, B.S. Kumari, K.V. Rao and Y.T. Prabhu, *Int. J. Curr. Eng. Technol.*, **4**, 2347 (2014).
39. S. Ranwa, P.K. Kulriya, V.K. Sahu, L.M. Kukreja and M. Kumar, *Phys. Lett.*, **105**, 213103 (2014); https://doi.org/10.1063/1.4902520
40. R. Gao, Z. Ying, W. Sheng and P. Zheng, *Mater. Lett.*, **229**, 210 (2018); https://doi.org/10.1016/j.matlet.2018.07.018
41. A.V. Patil, C.G. Dighavkar, S.K. Sonawane, S.J. Patil and R.Y. Borse, *Sens. Transd. J.*, **9**, 11 (2010).
42. P.P. Sahay and R.K. Nath, *Sens. Actuators B Chem.*, **133**, 222 (2008); https://doi.org/10.1016/j.snb.2008.02.014
43. A.R. Raju and C.N. Rao, *Sens. Actuators B Chem.*, **3**, 305 (1991); https://doi.org/10.1016/0925-4005(91)80021-B
44. Z.-P. Sun, L. Liu, L. Zhang and D.-Z. Jia, *Nanotechnology*, **17**, 2266 (2006); https://doi.org/10.1088/0957-4484/17/9/032
45. K.-S. Choi and S.-P. Chang, *Mater. Lett.*, **230**, 48 (2018); https://doi.org/10.1016/j.matlet.2018.07.031